Technical Physics, Vol. 47, No. 2, 2002, pp. 238–243. Translated from Zhurnal Tekhnicheskoĭ Fiziki, Vol. 72, No. 2, 2002, pp. 99–104.

SURFACES, ELECTRON AND ION EMISSION

Production and Properties of Metal–Carbon Composite Coatings with a Nanocrystalline Structure

S. A. Shiryaev, M. V. Atamanov, M. I. Guseva, Yu. V. Martynenko, A. V. Mitin, V. S. Mitin, and P. G. Moskovkin

Russian Research Center Kurchatov Institute, pl. Kurchatova 1, Moscow, 123182 Russia

e-mail: martyn@nfi.kiae.ru

Received May 4, 2001

Abstract—It is suggested to produce metal–carbon composite coatings by magnetron sputtering of mosaic cathodes, which are Group IV, V, and VI metals. The mosaic structure of the cathode elements are computer-optimized for each of the metals. Reflection electron diffraction studies show that the coatings have the amorphous or nanocrystalline structures, which are thermally stable. The coatings offer specific physical properties, in particular, low friction factor and high hardness. © *2002 MAIK "Nauka/Interperiodica".*

INTRODUCTION

Modern methods for solid surface modification, such as ion implantation and magnetron sputtering, as well as their combination, allow one to alter the surface properties of structural materials in a wide range. Coatings made of transition metal (Groups IVA–VIA) carbides with the face-centered cubic (fcc) lattice are of particular interest, because this lattice is typical of metals characterized by high hardness, excellent high-temperature strength, and good corrosion resistance.

In this work, we synthesize the coatings of transition metal carbides (TiC, Ta_2C, Ta_3C_2, CrC, NbC, Mo_2C, and (TiC)N(Mo_2C)N) by co-sputtering of the mosaic cathodes. The cathodes, metal–graphite mixtures, were sputtered by Ar^+ ions or by an $Ar^+ + N^+$ mixture in the magnetron plasma.

Magnetron sputtering is widely used for the deposition of various coatings [1], in studying composite coatings. In the latter case, the cathode is usually made from an alloy of necessary composition, which is sputtered in the magnetron [2].

We suggest to apply composite coatings by using a mosaic cathode. The mosaic structure of the cathode (target) is selected in such a way as to provide coatings of uniform composition.

THEORETICAL GROUNDS OF FILM DEPOSITION USING MAGNETRON SPUTTERING OF A MOSAIC CATHODE

If the cathode is inhomogeneous, the erosion of the different materials proceeds at a various rate due to a difference in the sputtering coefficients. As a result, the materials with a higher sputtering coefficient turn out to be farther from the plasma than those with a lesser sputtering coefficient. The ion current density on the cathode is equal to the number of ions incident on a unit area per unit time:

$$j = nv_T/4, \tag{1}$$

where v_T is the ion thermal velocity and n is the plasma density.

The ion current decreases at the recessed cathode parts, i.e., at the materials with the higher sputtering coefficient. Indeed, the plasma boundary is located at the level of the highest cathode point along the magnetic line of force. Downward, i.e., toward the cathode, the plasma density n rapidly decreases, because plasma electrons are magnetized and be deflected from the plasma boundary by no more than the Larmor radius

$$r_L = mv_e/eB,$$

where m is the electron mass, v_e is the electron velocity, e is the electron charge, and B is the magnetic field.

The ions and the electrons cannot be spaced more than the Debye length apart. The Debye length is given by

$$r_D = (T/4\pi ne^2)^{1/2},$$

where T is the plasma temperature.

Therefore, the characteristic distance of plasma density decrease can be estimated as

$$r_0 = r_L + r_D.$$

As a result, the erosion rates of the different cathode materials become equal. In this case, the material surface moves due to erosion with a velocity

$$u = Yj/N, \tag{2}$$

where Y is the sputtering coefficient and N is the volume atom concentration.

1063-7842/02/4702-0238$22.00

Thus, assuming that the ion velocities do not depend on the distance from the cathode, we obtain the following condition for the erosion of two materials:

$$S_1 n(x_1)/N_1 = S_2 n(x_2)/N_2, \quad (3)$$

where x_1 and x_2 are the surface coordinates of the first and second materials, respectively, along the axis normal to the surface.

Knowing the dependence $n(x)$, one can calculate from Eq. (3) the displacement $\Delta x = |x_1 - x_2|$ of the surfaces for the same erosion rates.

If the plasma-facing surfaces of different materials constituting the target used for the deposition of multicomponent coatings are coplanar, the ratio of the components being deposited will first be proportional to the product of the area of sputtering by the sputtering coefficient. As time passes, the erosion process becomes steady-state, the erosion rates of all the components become equal, and the ratio of the components is proportional to the area of sputtering on the cathode. The transient period of the erosion process is

$$\tau = \Delta x/\Delta u, \quad (4)$$

where $\Delta u = |u_1 - u_2|$ is the difference in the rates of surface sputtering.

Therefore, in practice, the cathode composition should be selected, starting from the equal erosion rates for all components. However, the coating deposited for the early period of time τ should be removed. Subsequently, when the values of the surface displacement Δx for the components with higher sputtering coefficients are accurately determined experimentally, these components can be recessed at once by Δx when manufacturing the cathode. In our conditions, $r_0 \approx 10^{-4}$ m and $\tau = \Delta x/\Delta u \approx 10^3$ s.

A computational code has been developed to simulate the percentage of the components in the film deposited and the film thickness. The code makes it possible to analyze the film deposition process when the targets of different geometry and composition are employed.

A mosaic target used in the simulation is composed of base material *1* and overlying islands made of materials *2* and *3* (Fig. 1). However, our model applies to targets consisting of an arbitrary number of components.

To determine the percentage of the components in the coating, the contributions from each of the target islands were calculated and then summed. The calculations, using several angular distribution functions for particles sputtered, showed that the distribution of particles deposited slightly depends on the distribution function; therefore, the distribution function in the form $f(\Theta) = \cos\Theta$ was used.

The distribution of the components in the film depends on the distance h between the target and the plane of deposition. Therefore, the calculations were performed for different values of h. The results are given in Figs. 2 and 3, where the distribution of one component in the film is shown. It is seen that, at a small distance from the target, the components are deposited nonuniformly. The point is that, at a small distance from the substrate, the material of each of the islands is deposited directly underneath the island. As the distance increases, the distribution becomes more uniform. At the same time, the amount of the material reaching the substrate decreases. Therefore, the exposure time should be increased to obtain a coating of a desired thickness. From geometric considerations, one can conclude that the material distribution in the film becomes uniform when the target–film distance R exceeds the island spacing. At the same time, the density of the deposit is proportional to the ratio of the film area S to R^2. Hence, to minimize the deposition time, the substrate should be placed nearer to the target.

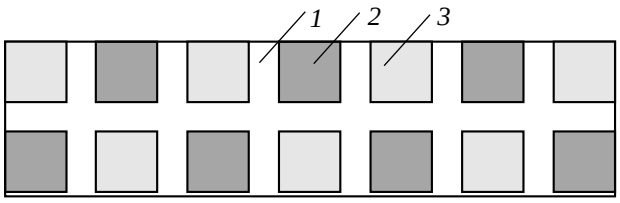

Fig. 1. Geometry of the composite target used in simulation.

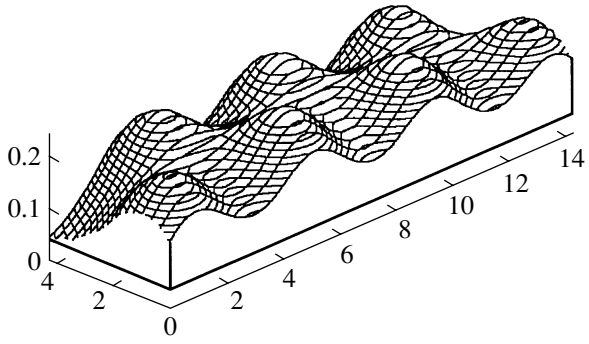

Fig. 2. Concentration of one component in the coating for the coating–cathode distance $h = 2$ cm.

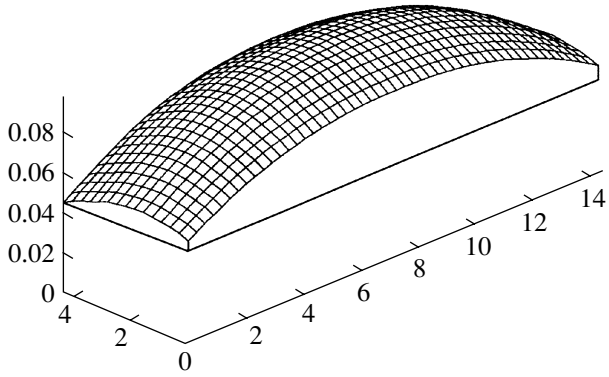

Fig. 3. The same for $h = 6$ cm.

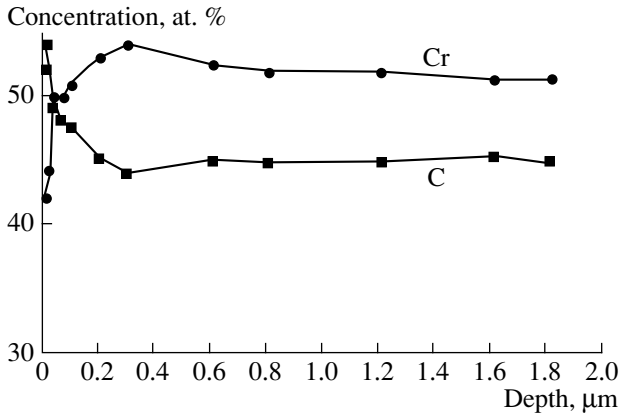

Fig. 4. Cr and C distributions in the coating. The chromium and graphite areas on the cathode relate as 50 : 50%.

Note also that the film thickness near the edges is smaller, which should be taken into account when arranging the substrates. The simulation showed the following: (1) the magnetron sputtering of the mosaic target provides the deposition of the homogeneous films; (2) to produce a film of uniform component distribution over the surface, the substrate surface should be placed at a distance far exceeding (about 3 times) the distance between the islands; (3) as the distance increases, the number of target atoms reaching the film decreases, so that the exposure time must be increased to obtain the film of a desired thickness.

EXPERIMENTAL

The experiments were carried out using a Vita ion accelerator equipped with a high-energy ion source, a plasma accelerator, and a magnetron. Metal–graphite compositions were used as the cathode. The metals were tantalum, molybdenum, niobium, vanadium, chromium, zirconium, titanium, and oxygen-free copper. The refractory metals were prepared by vacuum melting. We also used high-purity fine-grain graphite of density $1.81–1.86 \times 10^3$ kg/m^3, which can be mechanically treated and polished.

To perform complex investigations, the coating was deposited onto different metals; glass; ceramics; and hard-alloy foils, plates, and beads with a polished surface. The TiC and TiCN, NbC, WC, CrC, MoC, and MoCN coatings were synthesized by sputtering the cathodes made of corresponding metals with graphite inclusions by Ar^+ ions or an $Ar^+ + N^+$ mixture.

Depending on the material to be sputtered, the cathode voltage was varied from 400 to 600 V; the current, in the range of 5–10 mA.

Before the deposition, the substrates were cleaned by a high-energy (300 eV) Ar^+ ion beam extracted from the plasma accelerator. After the deposition, the composition and the thickness of the coatings were studied with Rutherford backscattering.

The phase composition and the structure of the coatings were examined by high-energy electron diffraction with a transmission electron microscope and an electron diffractometer, X-ray diffraction, X-ray photoelectron spectroscopy, Auger electron spectroscopy, scanning electron microscopy, X-ray microspectral analysis with an SEM, and optical microscopy.

The coating thickness was estimated on the cleavage surface using a scanning electron microscope and a profilometer.

The coating adhesion to the substrate was tested by a REVETEST standard automatic tester available from the LSRH using a Rockwell C indenter. The loading rate was 100 N/min; the indenter velocity, 10 mm/min. The coating microhardness was determined using a PMT-3 hardness meter and an MI-7 microscope under a load of 0.2–2.0 N.

The wear resistance of the coatings was determined by rubbing against a loosely fixed abrasive (diamond paste on a thick paper) of granulometric composition $(10–15) \times 10^{-6}$ m on a friction machine at a constant load of 26 Pa. The coating thickness was found to be $(3–25) \times 10^{-6}$ m. The wear resistance was estimated

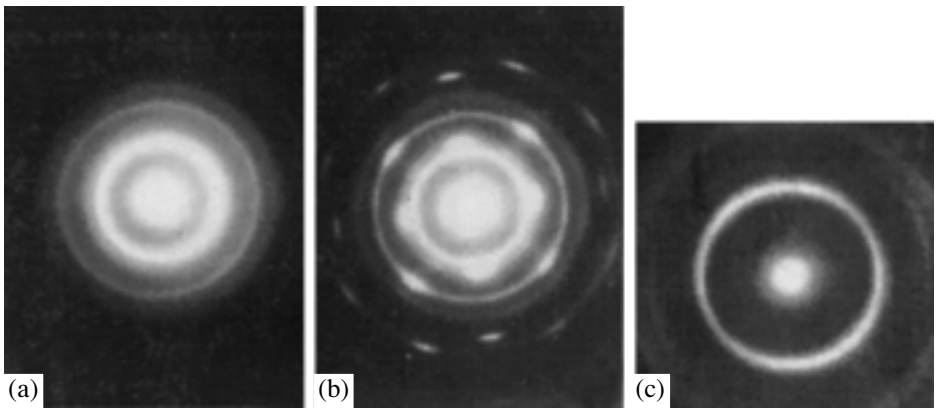

Fig. 5. Diffraction patterns for the (a) Ta_2C, (b) TaC, and (c) Ta_3C_2 in the Ta–C coating.

Composition and properties of coatings

Compound	Cathode composition, ratio Me : C over surface in %	Phase composition of coating (X-ray data), wt %	Lattice types and parameters, $\times 10^{-1}$ nm	Crystallite size, $\times 10^{-1}$ nm	Chemical composition, wt %	Microhardness H_V (0.2–1 H), GPa
(WG)	50W + 50C	$WC_{0.97}$ = 96.4 ± 0.4 C = 3.6 ± 0.4	hcp *a* = 2.907 *b* = 2.839	30–40		16.00–27.0 (~24)*
(7GTa) (13TaG)	50Ta + 50C	$TaC_{0.97–0.1}$ = 97.6 ± 0.4 C = 3.4 ± 0.4	fcc *a* = 4.44	60–80		15.30–27.00 (15.7)
(6MoG)	70Mo + 30C	Mo_2C = 67.6 ± 0.4 Mo = 32.4 ± 0.4 Closer to β-Mo_2C, high-temperature	hcp *a* = 3.01 *c* = 4.74	Texture 22–50	Mo(tot) = 77.6 + 2.3 C(tot) = 2.3 ± 0.3 Mo(fr) = 38.6 ± 2.3	13.00–30.00
(18MoG) (19MoG)	50Mo + 50C	$MoC_{0.95–1.0}$ = 95.6 ± 0.4 C = 4.2	fcc α-MoC *a* = 4.27	60–80	Mo(tot) = 82.6 ± 2.6 84.5 ± 0.6 C(tot) = 15.5 ± 0.6 16.2 ± 0.1 C(fr) = 1.4 ± 1.0 5.6 ± 1.5	18.00–31.00
(11NbC)	70Nb + 30C	Nb_2C	Hexagonal *a* = 3.115, *c* = 4.948	Texture 10–30	Nb(tot) = 2.6 ± 0.7 C(tot) = 6.07 ± 1.5	23.00–29.00 (24)
(NbG)	50Nb + 50C	$NbC_{0.95–1.0}$	fcc *a* = 4.436	Texture 20–50	Nb(tot) = 84.3 ± 3.0 C(tot) = 11.45 ± 0.8	18.90–23.00 (24)
(10GV)	50V + 50C	$VC_{0.85–0.88}$	fcc *a* = 4.188	15–50	V(tot) = 84.3 ± 3.0 C(tot) = 9.5 ± 0.5	13.00–26.00 (28)
(8GCr)	50Cr + 50C	Cr_3C + Cr Closer to Cr_6C phase	Rhombic *a* = 2.86, *b* = 5.58, *c* = 11.48	80–120	Cr(tot) = 84.3 ± 2.8 C(tot) = 13.4 ± 0.2 C(fr) = 0.59 ± 0.05	17.00–27.00
(2TiG)	50Ti + 50C	$TiC_{0.95–0.98}$ = 98.5 ± 0.4	Cubic, type V-1 4.330	Texture 111 30–50		21.50–37.40 (29.3)
(3TiG)	80Ti : 20C	$TiC_{0.5–0.6}$ = 68.6 ± 0.4 Ti = 31.4 ± 0.4	Cubic, type V-1 4.334	80–120		11.00–22.00
(4ZrG)	50Zr : 50C	$ZrC_{0.9–0.95}$ = 96.5 ± 0.4	Cubic, type V-1 4.677	50–60		18.50–30.00 (28.6)
(5ZrG)	80Zr : 20C	$ZrC_{0.5–0.6}$ = 76.5 ± 0.4 Zr = 23.5 ± 0.4	Cubic, type V-1 4.683	Texture 120–180		10.00–21.00

Note: tot, total content; fr, in free state; * refers to tabulated value.

from the rate of linear wear and friction track coloration.

The friction coefficient was determined using a sliding friction machine as follows: a coated rotating disk rubbed against an uncoated fixed ball under dry friction conditions in air.

The chemical composition of the coatings, i.e., the content of the metal and carbon in bound and free states, was determined by specially developed techniques with a Leco C-212 AH-7529 analyzer.

The thermal oxidation resistance in air and in a pure oxygen flow was tested by the method of thermogravimetric oxidation using a Setaram instrument (France).

The corrosion resistance of the coatings was estimated electrochemically using a PS4 potentiostat by plotting anode potentiodynamic polarization curves at a

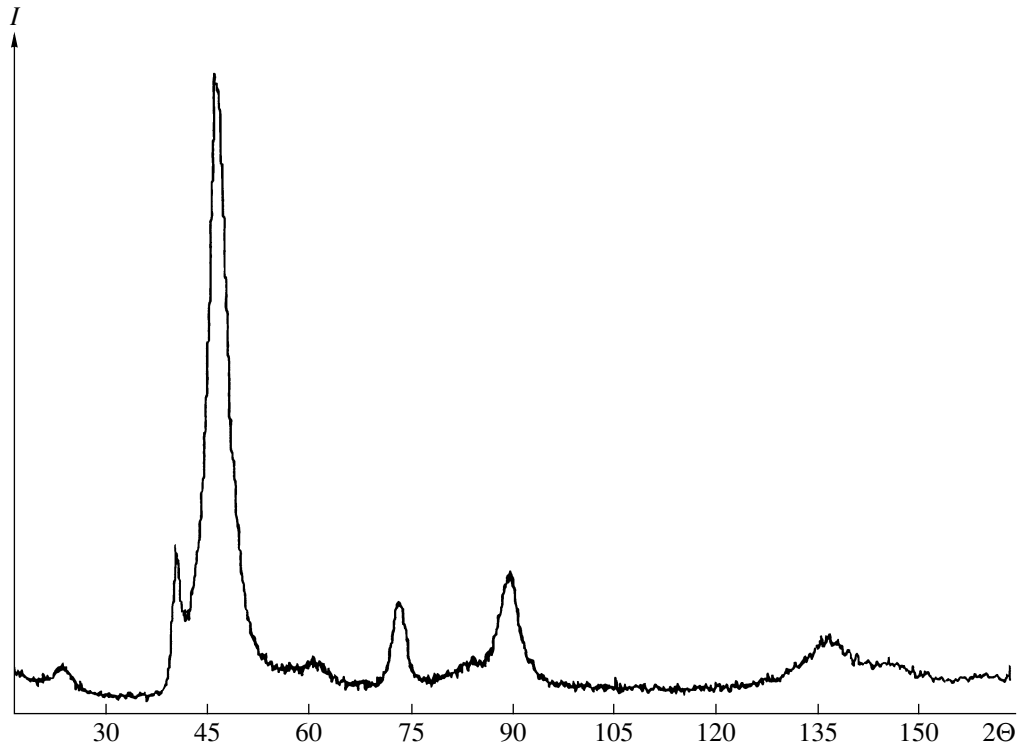

Fig. 6. X-ray reflections for the Mo–C coating. The phases are Mo_2C with a crystallite size of 4.8 nm, Mo_4C (5.1 nm), and a small amount of MoC (2.29 nm).

rate of 7.8 V/h in H_2SO_4 and HCl solutions at room temperature.

EXPERIMENTAL RESULTS

For discharge power densities from 5×10^5 to 11×10^5 W/m^2, we obtained smooth homogeneous condensates with metallic luster on different substrates. On the polished and glass substrates, the condensate had the specular surface, which is typical of refractory metal layers.

The investigation of the phase composition and the structure of the coating shows that when the mosaic cathode is sputtered, the metal and carbon atoms homogeneously mix to form carbides, if the metals interact with carbon, or pseudosolid carbon solutions in metals otherwise. All the Group IVA–VIA refractory metals studied in this work interact with carbon at temperatures no more than 473 K to form carbide phases, including high-temperature phases (see table). The formation of these phases is also confirmed by photoelectron energy spectrum analysis. The variation in the element composition of the coating across the depth is typical of almost all of the compositions. The Auger spectroscopy data for Cr–C, Ta–C, and Mo–C demonstrate that ion etching causes the C concentration to decrease and the metal concentration to increase (Fig. 4). Apparently, this results from graphite diffusion into the coating and its segregation at the surface.

The measurement of residual stress in the 6MoG, 19MoG, and 8GCr samples (see table) by the X-ray diffractometer equipped with a special ψ attachment shows that in the Mo phase, compressive stresses in the coating plane are $\approx$0.3 GN/m^2 (6MoG), while in MoC phases, they are 0.19 GN/m^2 (19MoG). In both cases, the coatings were deposited on carbon ball bearing steel.

The estimation of the adhesion for metal–carbon coatings as a whole (both qualitative and quantitative) shows that the highest adhesion (about the mean carbide tensile strength, 0.18–0.25 GPa; incomplete detachment: film islands remain on the substrate) is observed for the ductile substrates (such as copper, nickel, low-carbon and stainless steel). The adhesion was 1.5–2 times lower for the substrates made of the hard allow, high-speed and ball bearing steel, as well as of glass and ceramics. This is especially true for the coatings of a thickness $>5 \times 10^{-6}$ m.

The reflection and transmission electron microscopy studies of the coating surface confirm the presence of the ultrafine-grain nearly amorphous structure, as evidenced by the diffraction patterns (Fig. 5).

X-ray reflections for the Mo–C coating are shown in Fig. 6. Their identification shows that the coating is multiphase, containing Mo_2C with a crystallite diameter of 4.8 nm, Mo_4C (5.1 nm), and a small amount of

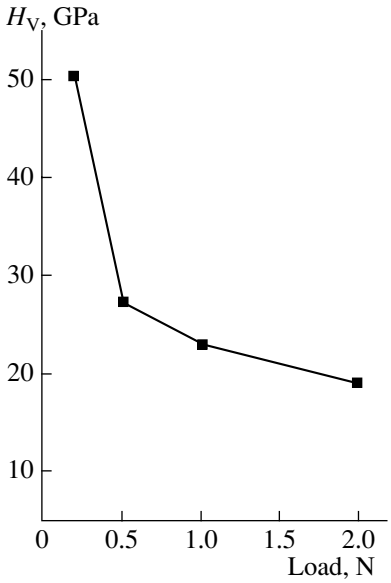

Fig. 7. Microhardness vs. load for the Mo–C coating.

MoC (2.29 nm). One can conclude that the molybdenum carbides have the nanocrystalline structure.

As the carbon content decreases and phases, such as Ta_2C, Nb_2C, and Mo_2C appear, i.e., when hcp MeC subcarbides form instead of the fcc MeC carbides (NaCl-like structure), the structure of coatings sharply changes. The lines 200, 220, and 111, which are typical of the fcc lattice with a parameter of 0.444 nm, are successively smeared. The ultrafine-grain nanocrystalline structure of the coatings provides high resistance to oxidation and corrosion. They also offer improved mechanical properties: hardness and wear resistance. The Mo–C coating is the hardest. For this coating, the microhardness as a function of load is shown in Fig. 7. The surface layer is superhard at a load of 0.2 N, H_V = 50 GPa.

The wear tests using a diamond paste showed the coatings with the composition $Me_2C + Me_{C_B}$ and $MeC + C_{C_B}$ offer the highest wear resistance.

Thus, it is shown that the co-sputtering of a metal and carbon provides their homogeneous mixing. The resulting deposits may contain both bound and free metal and carbon atoms. The coatings have the ultrafine-grain near-amorphous nanocrystalline structure, and this state is retained up to an annealing temperature of ≈1000 K.

In comparison with crystalline materials of this class, the metal–carbon coatings with the nanocrystalline structure offer higher corrosion resistance in a number of acids, higher oxidation resistance in air, lower friction coefficient, and higher wear resistance. The MoC coating is superhard (H_V = 50 GPa at 0.2 N).

ACKNOWLEDGMENTS

Yu.V. Martynenko and P.G. Moskovkin thank the Grant Council at the President of the Russian Federation and the Leading Scientific School Foundation (grant no. 00-15-96526) for the support.

REFERENCES

1. P. J. Kelly and R. D. Arnell, Vacuum **56**, 159 (2000).
2. J. Musil and J. Vicek, in *Proceedings of the 5th Conference on Modification of Materials with Particle Beams and Plasma Flows, Tomsk, 2000*, p. 393.

Translated by M. Astrov